Structural Engineering and Mechanics, *Vol. 63, No. 4 (2017) 497-507*
DOI: https://doi.org/10.12989/sem.2017.63.4.497

Seismic response of RC structures rehabilitated with SMA under near-field earthquakes

M.R. Shiravand[*1], A. Khorrami Nejad[1a] and M.H. Bayanifar[2b]

[1]*Department of Civil Engineering, Shahid Beheshti University, Tehran, Iran*
[2]*Department of Civil Engineering, Qazvin Branch of Islamic Azad University, Qazvin, Iran*

(Received December 1, 2016, Revised April 29, 2017, Accepted May 30, 2017)

Abstract. During recent earthquakes, a significant number of concrete structures suffered extensive damage. Conventional reinforced concrete structures are designed for life-time safety that may see permanent inelastic deformation after severe earthquakes. Hence, there is a need to utilize adequate materials that have the ability to tolerate large deformation and get back to their original shape. Super-elastic shape memory alloy (SMA) is a smart material with unique properties, such as the ability to regain undeformed shape by unloading or heating. In this research, four different stories (three, five, seven and nine) of reinforced concrete (RC) buildings have been studied and subjected to near-field ground motions. For each building, two different types of reinforcement detailing are considered, including (1) conventional steel reinforcement (RC frame) and (2) steel-SMA reinforcement (SMA RC frame), with SMA bars being used at plastic zones of beams and steel bars in other regions. Nonlinear time history analyses have been performed by "SeismoStruct" finite element software. The results indicate that the application of SMA materials in plastic hinge regions of the beams lead to reduction of the residual displacement and consequently post-earthquake repairs. In general, it can be said that shape memory alloy materials reduce structural damage and retrofit costs.

Keywords: shape memory alloy material; ductility; nonlinear time history analysis; residual lateral displacement; near-field earthquake; concrete structures

1. Introduction

In previous earthquakes, such as the ones in Michoacán, Mexico, in 1985 and Northridge, USA, in 1994, many structures had been destroyed and rebuilt following large permanent deformation. Similarly, in the Kobe earthquake in Japan (1995), 240,000 buildings had been destroyed. Damage caused by the Kobe earthquake was estimated to be around 50 to 100 billion dollars (Comartin *et al.* 1995). Consequently, there is a general agreement among researchers on the importance of residual displacement on seismic performance and post-earthquake functionality of RC structures. Recently, SMAs have found significant applications in civil engineering due to their unique ability to undergo large deformations, up to 8-10%, and return to their original shape by heating (shape memory effect, Fig. 1(a)) or through removal of load (super-elastic effect, Fig. 1(b)). Super-elastic bars are capable of regaining their original shape through a crystalline phase transformation under stress change when the phase transformation temperature is sufficiently below the operating temperature

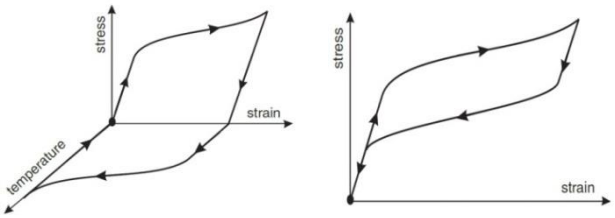

(a) Shape memory effect (b) Superelasticity

Fig. 1 SMA functional properties (Daghia *et al.* 2010)

(Des Roches *et al.* 2004).

Over the past few decades, there has been a significant amount of research dedicated to applications of SMAs to various civil structures, such as base isolation system, intelligent reinforced concrete beams, beam-column connections, steel frames, cable-stayed bridges and simply supported bridges as well as historical buildings. Many experimental studies (Saiidi and Wang 2006, Yusuf *et al.* 2008) evaluated the performance of RC structures with conventional steel reinforcement and SMA rebar in critical plastic hinge regions. They found that super-elastic SMA reinforcements could significantly improve the performance of RC structures by largely reducing the residual deformation. SMA reinforcements are capable of dissipating an adequate amount of energy. Alam and Youssef (2008) analytically studied the seismic behavior of super-elastic

∗Corresponding author, Assistant Professor
E-mail: m_shiravand@sbu.ac.ir
[a]Ph.D. Student
E-mail: a_khorraminejad@sbu.ac.ir
[b]M.Sc
E-mail: bayanifar.h@gmail.com

ISSN: 1225-4568 (Print), 1598-6217 (Online)

curves of steel-RC beam-column joints dissipated higher energy compared to that of SMA-RC beam-column joints; but the SMA-RC beam-column joint experienced lower residual deformation because of its capability in recovering from post-elastic strain. They also showed that the Paulay and Priestley equation was found to be the most appropriate one for prediction of plastic hinge length.

Alam *et al.* (2009) analytically explored the dynamic performance of an eight-story RC frame building reinforced with steel and SMA in its beam-column joints. The results showed that the main advantage of SMA-RC frame lies in its ability to reduce inter-story and top-story residual drifts. They found that steel-RC joints dissipated relatively higher amounts of energy compared to that of SMA-RC joints because of its large hysteretic loops. In case of steel RC frames, steel rebars experienced permanent deformation, which will cause difficulty in rehabilitation work. The costs involved, too, will also be high. On the other hand, in case of SMA RC frames, SMA rebar undergoes large inelastic strain due to a larger story-drift. However, this inelastic strain is potentially recovered, leaving negligible permanent deformation. Thus, the rehabilitation of SMA RC frames is expected to be easier and less costly compared to that of steel RC frames.

Abdulridha (2013) performed a study on SMA-reinforced concrete beams. The results showed that reversibility capability increased by over 93% for the SMA-reinforced beams compared to reinforced beams with conventional steel rebar. Shrestha *et al.* (2013) indicated that SMA-reinforced beams have the ability to decrease crack propagation by up to 89% compared to that of conventional reinforced beams without SMA rebar.

Nikbakht *et al.* (2014) analytically investigated the behavior of post-tensioned precast segmental bridge columns with super-elastic SMA bars. It was found that the bridge column with SMA bars compared with self-centering columns indicated higher energy dissipation, lower stiffness and strength up to 6.0% drift level. It was also evident from time history analyses that the SMA bars reduced the lateral seismic demand of precast segmental self-centering bridge columns. Shahnewaz and Alam (2015) performed incremental dynamic analysis (IDA) to investigate the seismic performance of RC shear wall with the application of SMA rebar at the plastic hinge location of the shear wall and the steel rebar was used for all other sections. The results showed that the SMA rebar significantly improved performance of the shear wall building and yielded higher collapse margin ratio (CMR) as compared to a conventional RC building.

Zafar and Andrawes (2015) investigated the performance of SMA-FRP rebars in RC MRF structures subjected to main shock-aftershock earthquake sequences and compared it with that of conventional steel rebars. Numerical results showed superior performance of SMA-FRP composite reinforced MRF in terms of dissipation of energy and accumulation of lower residual drifts. Increased demands from the effects of aftershock caused accumulation of residual drifts in steel reinforced frames, which are mitigated in SMA-FRP reinforced frame through re-centering capability.

The greater amount of damage and residual permanent displacement for structures located within the near-field earthquake zones pertains to the presence of long period pulse at the beginning of ground motion record. The damage is also caused by greater acceleration, higher velocity, more displacement and greater impact on structures compared to far-field earthquakes.

Hence, for damage reduction in near-field earthquakes, the earthquake's input energy can be controlled by some techniques like seismic isolation and dampers, or by using smart materials like shape memory alloys (SMAs) which can undergo large deformation without any failure or residual strain. This paper aims to evaluate the behavior of RC structures reinforced with SMA materials under near-field ground motions.

2. Basis of the study

Enhancing ductility and energy dissipation capacity are the most important concerns while designing seismic structures. In reinforced concrete structures, most of the formations of plastic hinges are at the beam ends through yielding of longitudinal reinforcement and concrete crushing in a zone with length of the beam depth from the column's face. The application of SMA rebars in the critical zones, such as plastic hinge regions, results in the reduction of the residual deformation in the aftermath of major earthquakes, as well as post-earthquake functionality of the RC structures. There is no need to rebuild or retrofit the structure.

It is evident from previous researches that the application of SMA reinforcement in plastic hinge regions had reduced the residual inter-story and roof drifts after a strong shaking, thanks to its unique shape recovery characteristics. However, observations from a damage investigation reported (by Decanini *et al.* 2005) after the 1999 Athens earthquake demonstrated that most of the severe damage occurred within 10 km from the source in the near-fault zone, and was mainly observed in the reinforced concrete frames and masonry buildings. They correlated this deficiency of RC buildings to the inadequate construction details and the imposed hysteretic energy demands on the RC buildings considering the structural system characteristics. They concluded that damage in the northern suburbs of Athens was due to a combination of different factors, such as local site amplification, topographic conditions, directivity and near-fault effects.

The earthquake's intensity depends on frequency content, soil type and distance of structure with seismic zone, which classifies earthquakes into two groups of near-field earthquakes and far-field earthquakes. Chopra *et al.* (2001) considered the ground motion recorded up to 10 km from the epicenter of the earthquake as near-field earthquakes. Also, the recorded ground motions with more than 50 km epicentral distance are termed far-field earthquakes. Latest researches have said that a high energy pulse is applied on the structure in a short time by the near-field ground motion. In this case, the structural behavior looks like the wave development on the elasto-plastic

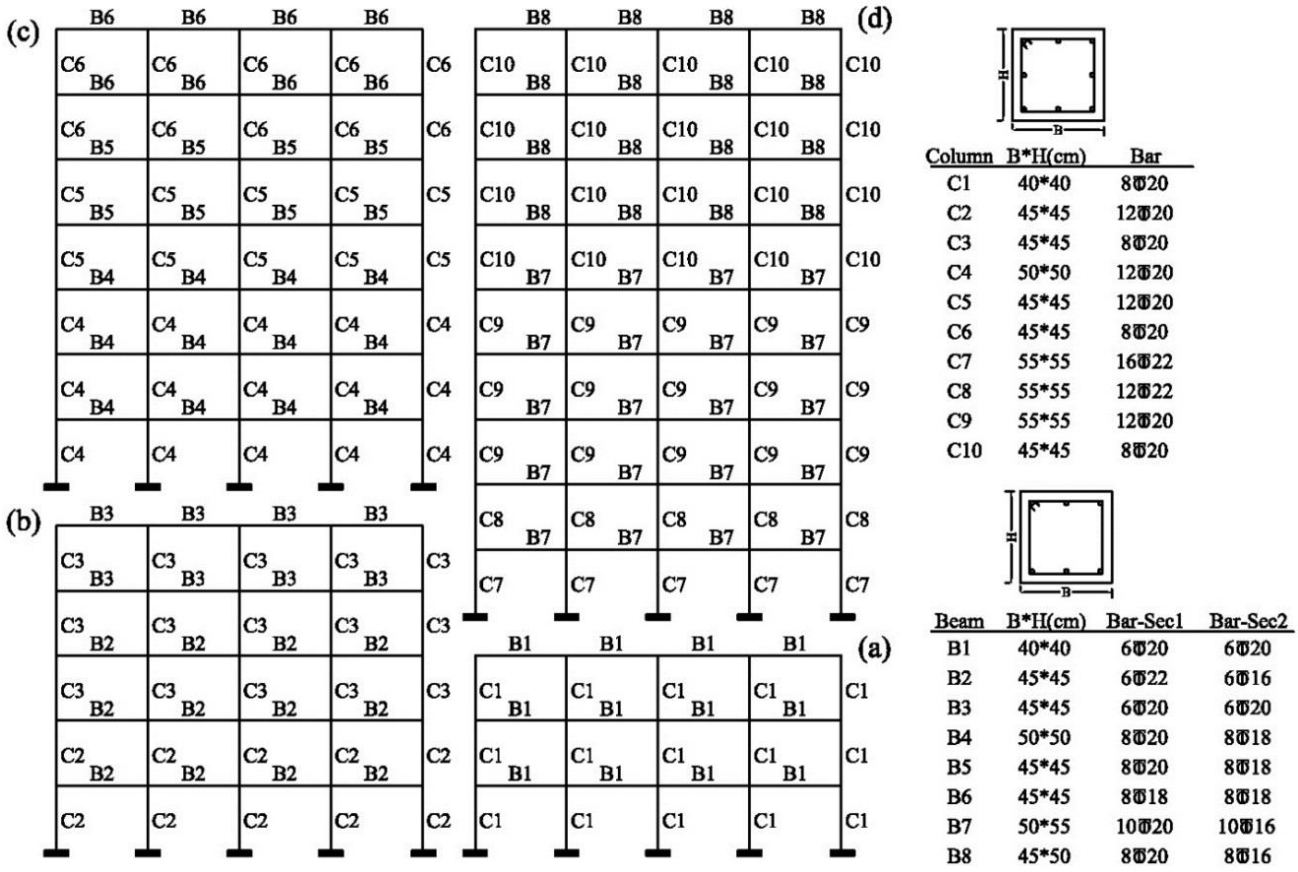

Fig. 2 General properties of the RC frames, (a) Three-story, (b) Five-story, (c) Seven-story, (d) Nine-story

environment (Decanini *et al.* 2000).

According to the promising application of SMAs in vulnerable regions of reinforced concrete structures, the study intends to investigate the efficiency of SMA RC frames in the pulse-like ground vibration of near-field earthquakes.

3. Numerical modeling of RC frames

3.1 Element and structural modeling

The finite element program, SeismoStruct software, with features including different material models like concrete, steel and SMA; different types of analysis, including dynamic and static time-history and the ability to take into account both geometric and material nonlinearities, were utilized to develop the analytical models. Four configurations of 2-D concrete frames with three, five, seven and nine stories were considered. Fig. 2 shows details of frame configuration and cross-sections of the beam and columns of RC frame models. Each frame has four spans with the same bay width of 4.5 m and the height of 3.2 m for all stories. Structures have been designed according to ACI 318-08. Dead and live loads considered are 33.11 kN/m and 8.83 kN/m respectively.

Two types of structural models are considered. The first type is the reinforced concrete frame with conventional steel rebar and the second one is the reinforced concrete frame with SMA rebar at the beam ends in plastic hinge zones in a specific length (L_p), and with conventional reinforcing in other parts. Columns are reinforced with conventional steel rebar in both types of frames. The plastic hinge length of the beams is considered through the empirical relations recommended by Paulay *et al.* (1992), Youssef *et al.* (2008), Saiidi and Wang (2006). The plastic hinges length (L_p), can be obtained with the help of the following equation.

$$L_p = 0.08(L) + 0.022\, d_{steel} \times f_y \quad (1)$$

where L_p is the plastic zone length, L is the net length of beam, d_{steel} is the diameter of rebar used in the member and f_y is the yield strength of steel bars.

According to Eq. (1), the plastic hinge length depends on the member's length, the yield stress, and the diameter of the steel bars. In this study, L_p for the steel bar with a diameter of 20 mm equals 536 mm, based on Eq. (1). Fig. 3 shows the layout of the reinforcement at the plastic hinge region for the retrofitted concrete frames with SMA. Coupling connectors suggested by Alam *et al.* (2010) are utilized for connection of the SMA bar to steel rebar.

Nonlinear beam-column elements with fiber sections were used to model the moment-resisting RC frame elements. The behavior of concrete material is modeled, based on the constitutive relationship by Mander *et al.* (1988) and the cyclic behavior by Martinez-Rueda and Elnashai (1997). In this model, the effects of transverse

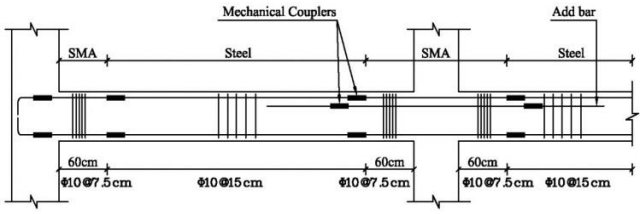

Fig. 3 Reinforcement details of the beams with SMA rebar (Alam *et al.* 2010)

Table 1 Material properties used in numerical models obtained from experimental tests

Material	Material Properties	Value
Concrete	Young's modulus	27.7 GPa
	Compressive Strength	35 MPa
	Ultimate strain	0.002
	Poission's ratio	0.2
Steel	Young's modulus	200 GPa
	Yield Stress	400 MPa
	Ultimate Strength	600 MPa
	Strain hardening	0.5 %
	Poission's ratio	0.3
SMA	Young's modulus	60 Gpa
	Austenite to Martensite start Stress	400 MPa
	Austenite to Martensite finish Stress	500 MPa
	Martensite to Austenite start Stress	300
	Martensite to Austenite finish Stress	100

reinforcement are considered a constant coefficient. The bilinear model is selected for the constitutive relationship of the steel material. The uniaxial behavior model presented by Auricchio and Sacco (1997) is considered for SMA materials. Table 1 shows detailed properties of each material utilized in developing the model.

3.2 Near-field seismic input and analysis

Twenty ground motion records from near-field earthquakes were chosen as seismic input for nonlinear time history analysis (Somerville *et al.* 1997). The earthquakes are chosen in the magnitude range of 6.7 to 7.5 (M_w) and at distances of 0 to 8.5 kilometers from the seismic source. The selected accelerograms have some features such as forward and backward directivity effect. The characteristics of near-field ground motion records are presented in Table 2. All the accelerograms are scaled, based on the peak acceleration of 0.35 g. Nonlinear time history dynamic analysis was performed on the structural models developed, utilizing the SeismoStruct software. The Hilber-Huges-Taylor (HHT) method is used for time integration in dynamic analysis.

4. Results and discussion

4.1 Drift angles demand

The average maximum drift angles of RC frames with and without SMA caused by the 20 near-field ground motion records are compared in Fig. 4. In the majority of the cases, the story drift angles of SMA RC frames are greater than the conventional RC frames. That stems from the greater stiffness of conventional RC frames in the elastic range compared to the SMA RC frame due to the greater modulus of elasticity of steel compared to SMA ($E_{SMA} \cong \frac{E_{steel}}{3}$). However, in some cases, the maximum drift angle of the SMA RC frames is less than the conventional RC frames. This is because of different kinds

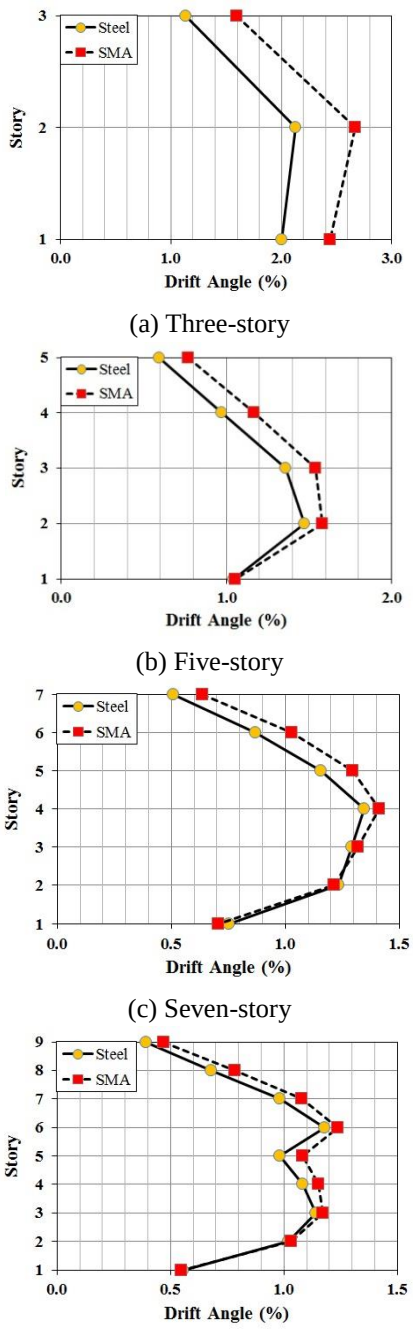

(a) Three-story

(b) Five-story

(c) Seven-story

(d) Nine-story

Fig. 4 Comparing the average drift angles of the RC and SMA RC frames

Table 2 Characteristics of the near-filed ground motion records (Somerville *et al.*, 1997) No.

	Record	Earthquake Magnitude (Mw)	Fault Type	Distance (km)	Directivity Effect
1	Loma Prieta, 1989, Los Gatos	7	Normal	3.5	Forward
2	Loma Prieta, 1989, Lex. Dam	7	Normal	6.3	Forward
3	C. Mendocino, 1992, Petrolia	7.1	Normal	8.5	Forward
4	Erzincan, 1992	6.7	Normal	2	Forward
5	Landers, 1992	7.3	Normal	1.1	Forward
6	Nothridge, 1994, Rinaldi	6.7	Normal	7.5	Forward
7	Nothridge, 1994, Olive View	6.7	Normal	6.4	Forward
8	Kobe, 1995	6.9	Normal	3.4	Forward
9	Kobe, 1995, Takatori	6.9	Normal	4.3	Forward
10	Tabas, 1978	7.4	Normal	1.2	Forward
11	Tabas, 1978	7.4	Parallel	1.2	Backward
12	Loma Prieta, 1989, Los Gatos	7	Parallel	3.5	Backward
13	Loma Prieta, 1989, Lex. Dam	7	Parallel	6.3	Backward
14	C. Mendocino, 1992, Petrolia	7.1	Parallel	8.5	Backward
15	Erzincan, 1992	6.7	Parallel	2	Backward
16	Landers, 1992	7.3	Parallel	1.1	Backward
17	Nothridge, 1994, Rinaldi	6.7	Parallel	7.5	Backward
18	Nothridge, 1994, Olive View	6.7	Parallel	6.4	Backward
19	Kobe, 1995	6.9	Parallel	3.4	Backward
20	Kobe, 1995, Takatori	6.9	Parallel	4.3	Backward

of structural behavior of the SMA RC frame in elastic and inelastic ranges compared to the conventional RC frames. Steel and SMA have linear behavior in the strain values up to 0.2% and 10% respectively. Hence, by increasing the seismic force level, beam section with conventional steel bars yields faster compared to the beam section reinforced with SMA. Therefore, for some ground motion records, the seismic forces do not reach the level that causes yielding of SMA and stiffness of the SMA RC frame is greater than the stiffness of conventional RC frames. In such cases, the lateral drift angle of SMA RC frames is less than the conventional RC frames. In general, the use of SMAs results in the reduction of the structural stiffness and increases fundamental period and story drift angles.

As shown in Fig. 4, the drift angles of the three-story SMA RC frame have been increased on an average by about 22%, 27% and 44.6% in the first, second, and third floors compared to the RC frames. The average drift angles of the five-story SMA RC frame have shown an increase of about 4.6%, 12.5%, 16%, 22% and 29% in the first, second, third, fourth and fifth floors compared to the conventional RC frames. In the seven-story SMA RC frame, the incremental trend of the average drift angles observed in the 2nd to 7th floor are about 2.5%, 8.5%, 10%, 15%, 19% and 25% (except the first floor). The relative drift in the first floor had shown about 4% reduction. For the nine-story SMA RC frame, the average drift angles have been increased by about 3%, 5%, 9%, 12.5%, 6%, 9%, 14% and 17.5% in the second to ninth floors except the first floor, which has shown a 1.5% decrement.

It can be implied from these results that the application of SMA in the RC frames leads to greater drift angles, but by increasing the height of the structure, this increasing trend declines. In other words, utilizing SMA bars for low-rise RC frames that are subjected to near-field ground motion records is not efficient. On the other hand, all the drift ratios of SMA RC frames are less than the allowable story drift specified in the ASCE/SEI 7-10 (i.e., 2.5% for frames up to four floors and 2% for five floors and more), except the second floor of the three-story frame.

4.2 Residual drift angles and roof drift demand

The average residual drift angles for three, five, seven and nine story frames caused by the 20 near-field ground motion records are shown in Fig. 5. In conventional RC frames, the maximum residual drift angles of three-, five-, seven- and nine-story frames obtained are 2.6%, 1.02%, 0.61% and 0.55% respectively. However, in SMA RC frames, the maximum residual drift angles equal 0.15%, 0.15%, 0.07% and 0.003% respectively for three-, five-, seven- and nine-story frames. It can be concluded that the maximum residual drift angles of three-, five-, seven- and nine-story SMA RC frames decrease by about 94%, 85%, 89% and 100% compared to that of conventional RC frames. This is a clear indicator that reinforcing with SMAs reduces the residual drift angles noticeably in all RC frames regardless of their height. Also, there is evidence that SMA RC frames are capable of limiting the residual roof drift by utilizing the capability of super-elastic SMA rebars. As a case study, the roof lateral displacement time-histories under ground motion 2 is shown in Fig. 6. The SMA RC frames' roof drifts have been increased at the beginning of the time series because of the lower stiffness of SMA compared to steel; but the residual roof drift of SMA RC frame equals nearly zero at the end of the seismic motion.

4.3 Energy dissipation capacity

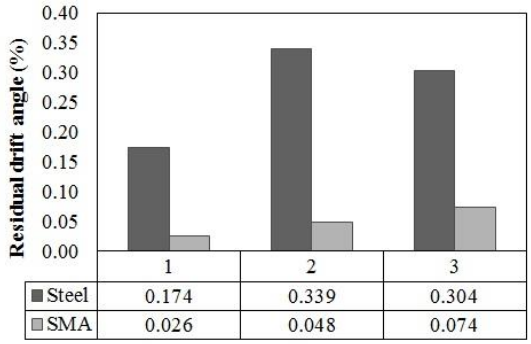

(a) Three-story

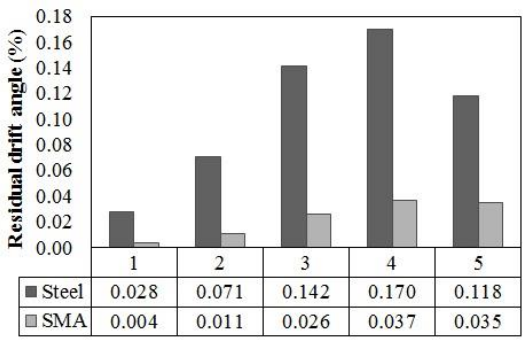

(b) Five-story

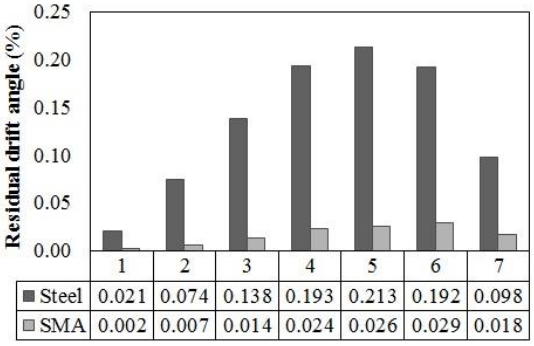

(c) Seven-story

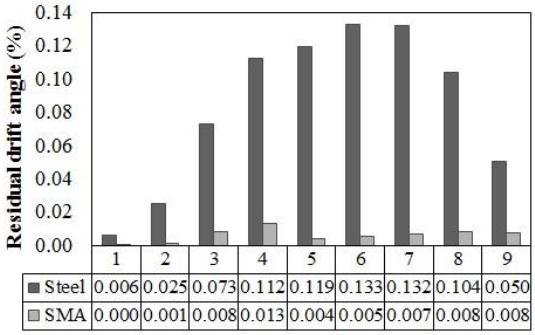

(d) Nine-story

Fig. 5 Comparing the average of residual drift angle for RC and SMA RC frames

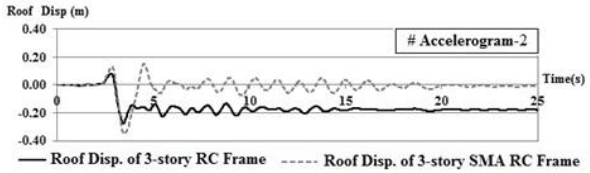

(a) Three-story

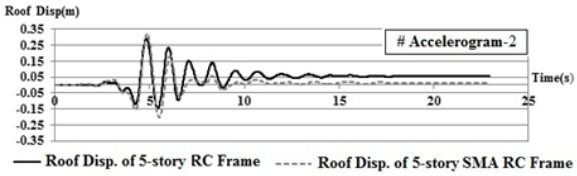

(b) Five-story

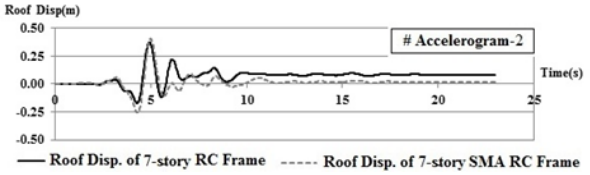

(c) Seven-story

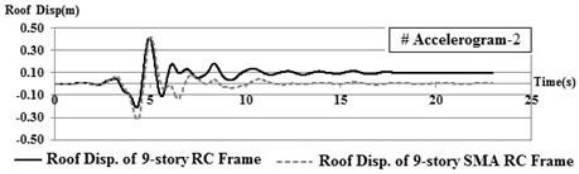

(d) Nine-story

Fig. 6 Roof lateral displacement due to ground motion record 2

A comparison of the energy dissipation capacities of the conventional RC and SMA RC frames is represented for ground motion records 5 and 7 in Fig. 7. Although RC and SMA RC frames have the ability to dissipate energy, in the majority of the cases, the dissipated energy of the RC frames is greater than the SMA RC frames. Regarding Fig. 7(a), the dissipated energy of the five-story and nine-story SMA RC frames have been decreased by about 32% and 40% respectively, unlike the three-story and seven-story SMA RC frames that have shown increases of about 40% and 10% compared to that of RC frames respectively. According to Fig. 7(b), the dissipated energy of the SMA RC frames have been decreased by about 75%, 70% and 50% for five-, seven- and nine-story frames respectively except for the three-story frame, which showed a 15% increase.

4.4 Damage assessment

MacGregor and Wight (2005) suggested strain values of 0.0025 to 0.05 as criteria for the failure assessment of the unconfined concrete crushing. The value of 0.0035 is considered the ultimate strain for unconfined concrete and 0.008 is relevant for confined concrete. Steel bar yielding, concrete cover crushing and concrete core crushing can be assumed as slight, moderate and extensive damage respectively.

The damage occurrence in RC frames and SMA RC frames caused by the ground motion record 1 is depicted in Figs. 8-11. With respect to Fig. 8, the reinforcing materials at both beam ends in the first and second floors and the steel bars of columns in the first floor have yielded. The noticeable difference between the damage that occurred in

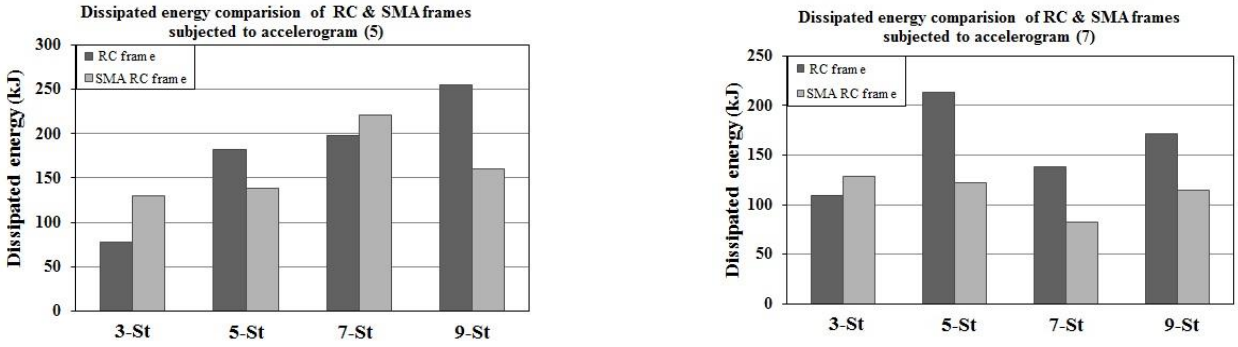

(a) Ground motion record #5 (b) Ground motion record #7

Fig. 7 Comparing the dissipated energy for RC frames and retrofitted RC frames with SMA

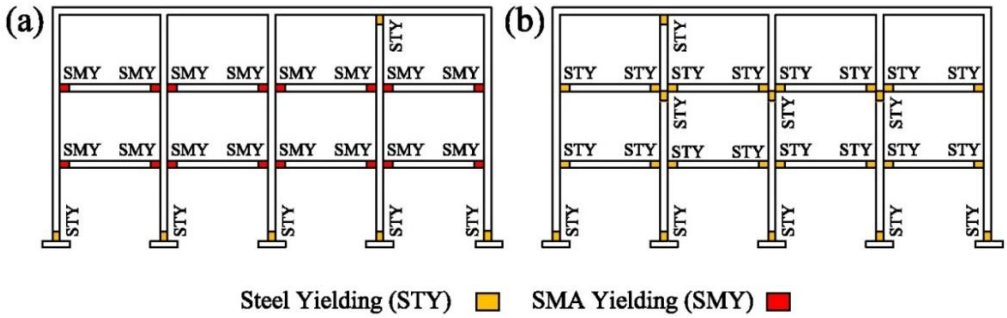

Fig. 8 Damage occurred in the three-story frame due to the ground motion record 1 (a) SMA RC frame (b) Conventional RC frame

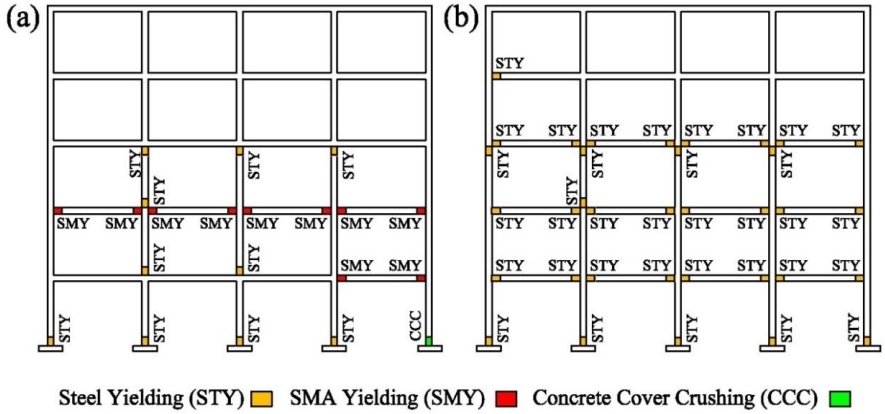

Fig. 9 Damage occurred in the five-story frame due to the ground motion record 1 (a) SMA RC frame (b) Conventional RC frame

the RC and SMA RC three-story frames are the connection elements of columns in the second floor. Unlike the SMA RC frame, reinforcing steel bars of RC frames in these connections have yielded. In the five-story frames, the damage that occurred in the SMA RC frame is significantly less than the RC frame (see Fig. 9). As can be seen in Fig. 10, all the reinforcing steel bars at the beam ends of the seven-story RC frames have experienced yielding in the first to fifth floors. But SMA rebars of the SMA RC frame have yielded in the first to fourth floors. Unlike the RC frame, the reinforcing rebars of SMA RC frame at the bottom of the columns of the first floor have yielded. Fig. 11 indicates that the nine-story SMA RC frames have experienced less damage compared to the conventional RC frame. From these results, it is apparent that the damage occurred in SMA RC frames is less than conventional RC frames. Also, the three-story SMA RC frames suffered more severe damage because of near-field ground motion.

4.5 Base shear distribution

Base shears of the conventional and retrofitted frames induced by 20 near-field ground motion records are shown in Fig. 12. Base shear is defined as the average of maximum base shears obtained from dynamic time history analyses. It can be inferred from the figures that the base shear had declined in the SMA RC frames compared to conventional RC frames regardless of their heights. Reduction of the base

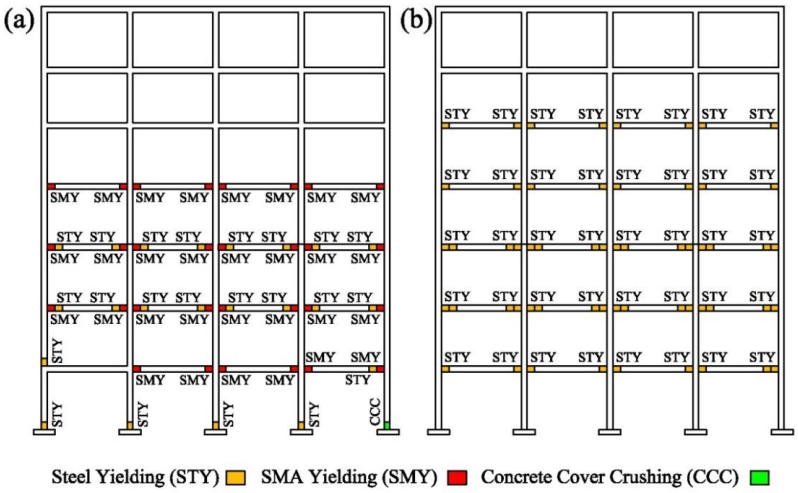

Fig. 10 Damage occurred in the seven-story frame due to the ground motion record 1 (a) SMA RC frame (b) Conventional RC frame

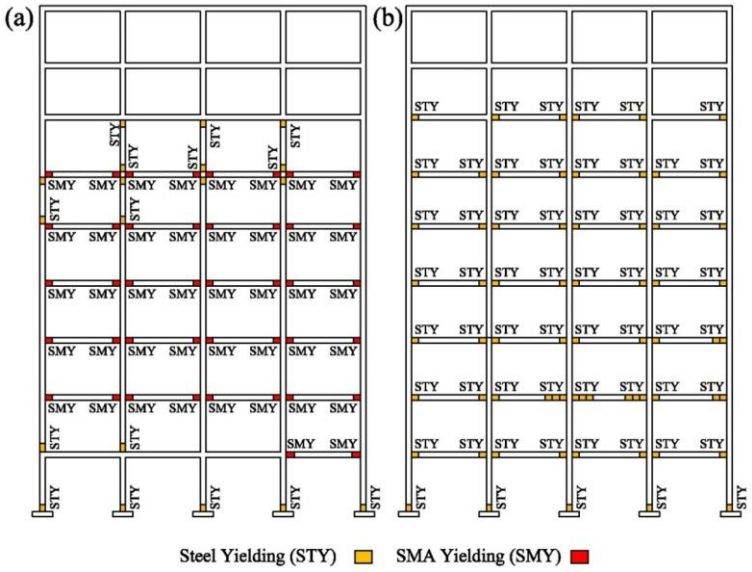

Fig. 11 Damage occurred in the nine-story frame due to the ground motion record 1 (a) SMA RC frame (b) Conventional RC frame

shear in the SMA RC frames pertains to the increase of the period and ductility (less stiffness compared to the RC frame), which leads to less input seismic forces. The three-story, five-story, seven-story, and nine-story SMA RC frame have shown 12%, 14%, 16.4% and 20.2% average reduction in base shear demand respectively compared to that of RC frame. It can be clearly seen that the application of SMA in RC frames yields base shear demand reduction as the height of the structure increases.

4.6 The stress-strain behavior of steel and SMA rebars

The stress-strain behavior curve of the reinforcing steel and SMA rebars are shown in Fig. 13 for highlighted point underground motion record #1. The steel rebar has yielded with a remarkable energy dissipation capacity. However, the maximum stress of the SMA rebar has reached the yield stress of SMA, and the flag-shape behavior can be observed. The strain time-histories of the outlined part of SMA RC and RC frames are shown in Fig. 14. The maximum strain in SMA and steel rebar are 0.0125 and 0.01 respectively. The increase in the SMA rebar's strain results from less stiffness (less elasticity modulus) compared to that of the steel rebar. It is obvious that the residual strain of the SMA rebar is much less than the steel rebar and approximately equals zero by utilizing the recentering capability of super-elastic SMA rebars.

5. Conclusions

This study was undertaken to examine some characteristics of SMAs such as super-elasticity, energy dissipation capability and reduction in the residual strain ability under near-field ground motions. For this purpose,

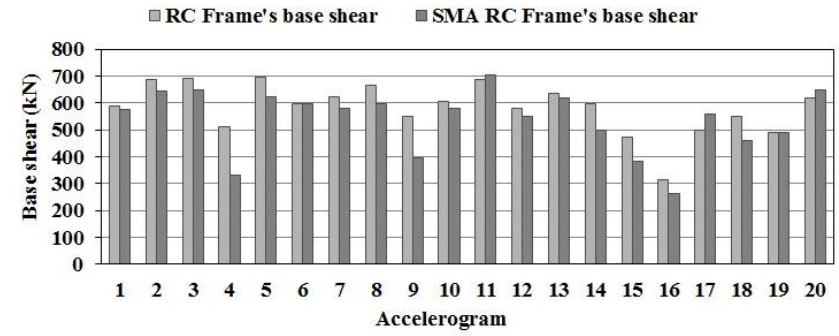

(a) Three-story

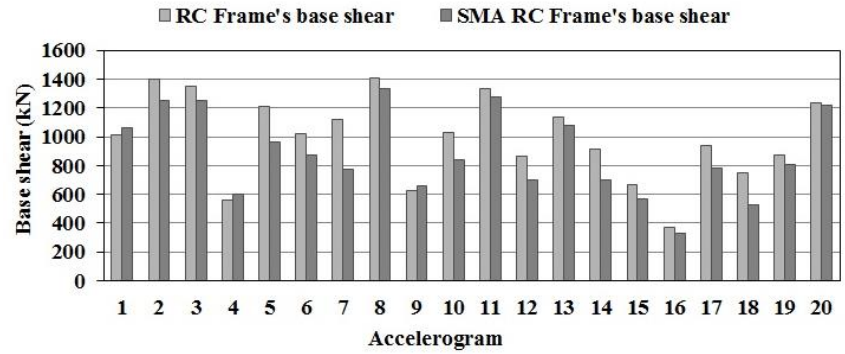

(b) Five-story

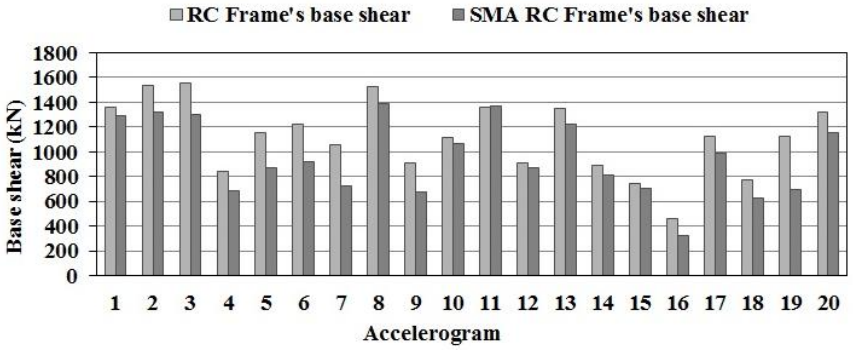

(c) Seven-story

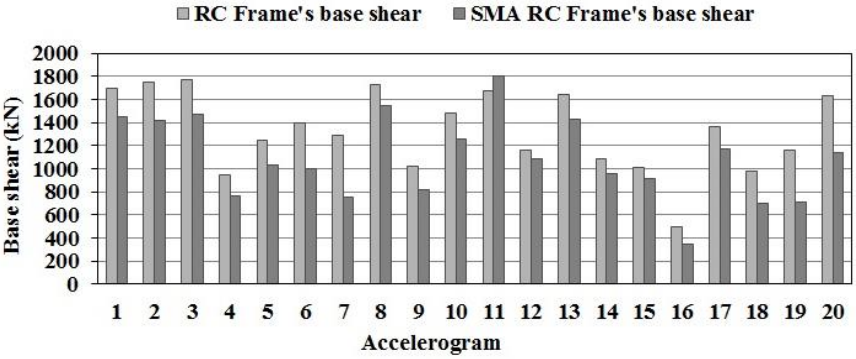

(d) Nine-story

Fig. 12 Comparing the base shear of the RC and SMA RC frames

nonlinear time history analyses have been conducted on concrete structures with three, five, seven and nine stories under 20 near-field ground acceleration time histories. Results imply that by increasing the height of the structure, the application of SMA rebars in RC frame leads to better performance due to the near-field seismic inputs. The major findings of this research can be summarized as follows:

- Using shape memory alloy materials lead to increase in the story drift angles from 5% to 45%. However, in some cases, the drift angle of the SMA RC frame is decreased compared to the RC frames due to the

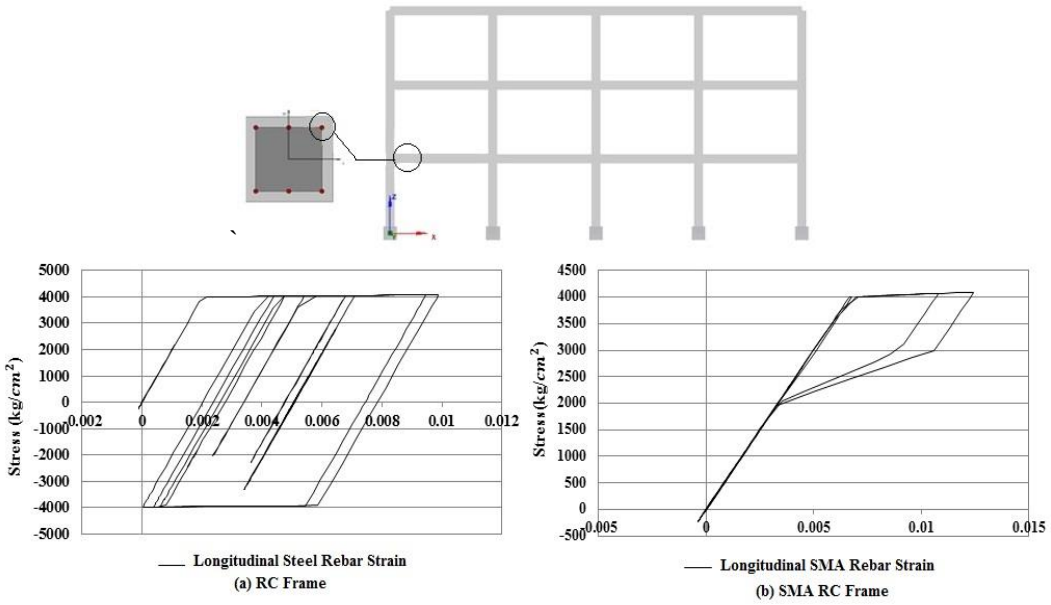

Fig. 13 The stress-strain behavior of the reinforcing steel and SMA rebars of the three-story concrete frames (a) RC frame (b) SMA RC Frame

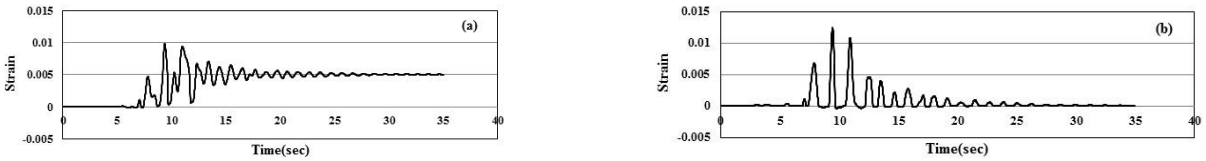

(a) RC frame (b) SMA RC Frame

Fig. 14 Strain time-histories of the reinforcing steel and SMA rebars of the three-story concrete frames

characteristics of near-field ground motions. In such cases, the seismic forces do not reach the yielding level of SMA rebars.

• In SMA RC frames, the residual drift angle is much less than conventional RC frames (about 100% compared to that of RC frames). This result indicates that by retrofitting the concrete frames with SMA, the normal operations of the structure will not be interrupted after near-field earthquakes.

• The three-story SMA RC frames subjected to near-field ground motion records suffered more severe damage. The damage that occurred in the five-, seven- and nine-story SMA RC frames is less than conventional RC frames. In other words, the failure rate in the SMA RC frame had declined.

• Base shear of the SMA RC frames under near-field earthquake records is reduced in the range of 12% to 20% compared to RC frames regardless of their height.

• Both the RC and the SMA RC frames have the ability to dissipate seismic energy. But in the majority of the cases, dissipated energy of the conventional RC frames is higher than the SMA RC frames.

References

Abdulridha, A., Palermo, D., Foo, S. and Vechi, F.J. (2013), "Behavior and modeling of superelastic shapememory alloy reinforced concrete beams", *Eng. Struct.*, **49**, 893-904.

ACI 318-08 (2008), Building Code Requirements forStructural Concrete (ACI 318-08) and Commentary, American Concrete Institute.

Alam, M., Nehdi, M. and Youssef, M. (2008), "Analytical prediction of the seismic behaviour of superelastic shape memory alloy reinforced concrete elements", *Eng. Struct.*, **30**, 3399-3411.

Alam, M., Nehdi, M. and Youssef, M. (2009), "Seismic performance of concrete frame structures reinforced with superelastic shape memory alloys", *Smart Struct. Syst.*, **5**(5), 565-585.

Alam, M., Youssef M. and Nehdi M. (2010), "Exploratory investigation on mechanical anchors for connecting SMA bars to steel or FRP bars", *Mater. Struct.*, **43**(S1), 91-107.

American Society of Civil Engineers (2010), "Minimum design loads for buildings and other structures", ASCE/SEI 7-10.

Auricchio F. and Sacco E. (1997), "A superelastic shape-memory-alloy beam model", *J. Intel. Mater. Syst. Struct.*, **8**(6), 489-501.

Chopra, A.K. and Chintanapakdee, C. (2001), "Comparing response of SDF systems to near-fault and far-fault earthquake motions in the context of spectral regions", *Earthq. Eng. Struct. Dyn.*, **30**(12), 1769-1789.

Comartin, C., Greene, M. and Tubbesing, S. (1995), "The Hyogo-Ken Nanbu earthquake preliminary reconnaissance report", Earthquake Engineering Research Institute, Oakland, CA

Daghia, F., Giammarruto, A. and Pascale, G. (2010), "Combined use of FBG sensors and SMA actuators for concrete beams repair", *Struct. Control Hlth. Monit.*, **18**, 908-921.

Decanini, L., Liberatore, L., Mollaioli, F. and De Sortis, A. (2005), "Estimation of near-source ground motion and seismic

behaviour of RC framed structures damaged by the 1999 Athenes earthquake", *J. Earthq. Eng.*, **9**(5), 609-635.
Decanini, L., Mollaioli, F. and Saragoni, R. (2000), "Energy and displacement demands imposed by near-source ground motions", *Proceedings of the 12th World Conference on Earthquake Engineering*, January.
DesRoches, R., McCormick, J. and Delemont, M. (2004), "Cyclic properties of superelastic shape memory alloy wires and bars", *J. Struct. Eng.*, **130**(1), 38-46.
Fugazza, D. (2003), "Shape-memory alloy devices for earthquake engineering: Mechanical properties, constitutive modeling and numerical simulations", Master's Thesis, University of Pavia, Italy.
Ghobarah, A. (2004), "On drift limits associated with different damage levels. in International workshop on performance-based seismic design", Dept. of Civil Engineering, McMaster University
MacGregor, J. and Wight. J. (2005), *Reinforced Concrete: Mechanics and Design*, 4th. Upper Saddle River, NJ, USA, Prentice Hall
Mander, J.B., Priestley, M.J. and Park, R. (1988), "Theoretical stress-strain model for confined concrete", *J. Struct. Eng.*, **114**(8), 1804-1826.
Martínez-Rueda, J.E. and Elnashai, A. (1997), "Confined concrete model under cyclic load", *Mater. Struct.*, **30**(3), 139-147.
Nikbakht, E., Rashida, K., Hejazi, F. and Osmana, S.A. (2014), "Application of shape memory alloy bars in self-centring precast segmental columns as seismic resistance", *J. Struct. Infrastr. Eng.*, **11**(3), 297-309.
Paulay, T. and Priestley M. (1992), "Seismic design of reinforced concrete and masonry structures", *J. Wiley & Sons, INC*, USA.
Saiidi, M.S. and Wang, H. (2006), "Exploratory study of seismic response of concrete columns with shape memory alloys reinforcement", *ACI Struct. J.*, **103**(3), 436-443.
SeismoSoft (2013). SeismoStruct. "A computer program for static and dynamic nonlinear analysis of framed structures", www.seismosoft.com.
Shahnewaz, M. and Alam, M.S. (2015), "Seismic performance of reinforced concrete wall with superelastic shape memory alloy rebar", *Structures Congress 2015*, 2230-2240.
Shrestha, K.C., Araki, Y., Nagae, T., Koetaka, Y., Suzuki, Y., Omori, T., Sotou, Y., Kainuma, R. and Ishida, K. (2013), "Feasibility of Cu-Al-Mn superelastic alloy bars as reinforcement elements in concrete beams", *Smart Mater. Struct.*, **22**(2), 025025.
Somerville, P.G. and Venture, S.J. (1997), "Development of ground motion time histories for phase 2 of the FEMA/SAC steel project", SAC Joint Venture.
Youssef, M., Alam, M. and Nehdi, M. (2008), "Experimental investigation on the seismic behavior of beam-column joints reinforced with superelastic shape memory alloys", *J. Earthq. Eng.*, **12**(7), 1205-1222.
Zafar, A. and Andrawes, B. (2015), "Seismic behavior of SMA-FRP reinforced concrete frames under sequential seismic hazard", *Eng. Struct.*, **98**, 163-173.

PL